Computing positron annihilation in polyatomic gases: An exploratory study

F. A. Gianturco,* T. Mukherjee,† and A. Occhigrossi
Department of Chemistry, The University of Rome, Cittá Universitaria, 00185 Rome, Italy
(Received 4 December 2000; published 20 August 2001)

The rates of positron annihilation in molecular gases are known to depend on the nanoscopic structural features of the ambient molecules. The aim of the present study is to explore the possible relationships that exist between some of the most salient molecular structural features and the ensuing positron annihilation rates at room temperature. Quantum dynamical calculations are applied to a broad variety of polyatomic targets using a parameter-free model interaction with the impinging positrons. The Z_{eff} values, as well as the integral elastic cross sections, are computed for such systems over the relevant range of collision energies. The dynamical treatment is shown to yield realistic values for the cross sections and to produce Z_{eff} values whose agreement with the few existing measured data varies greatly from one system to another.

DOI: 10.1103/PhysRevA.64.032715 PACS number(s): 34.85.+x

I. INTRODUCTION

The annihilation of low-energy positron beams in molecular gases, always a process of fundamental interest in atomic and molecular physics [1], has received considerable attention in the last few years because of the expanded experimental capabilities that have improved both the quality of the data and the intensity of the positron beams available for the measurements [2,3]. Thus, stored positrons are providing a broadening of the experiments that have become available and the generation of collimated positron beams with narrow energy spreads is suggesting a new class of scattering experiments [4].

The historical definition of the annihilation rate for positrons in a given ambient gas is usually given via a dimensionless parameter Z_{eff}

$$Z_{\text{eff}}=\frac{\lambda}{\pi r_0^2 c n}, \tag{1}$$

where λ is the observed rate of annihilation, r_0 the classical radius of a single electron, c the speed of light, and n the number density of atoms or molecules at the conditions of the ambient gas [5]. The above definition comes from the original formulation given by Dirac for a positron in a free electron gas. It represents a modification of it in the sense that the parameter Z_{eff} gives the effective number of electrons of the target molecule in the gas contributing to the annihilation process [6]. Such an approximation is, however, rather crude and is not really holding out even for atomic hydrogen [5]. It is even less realistic for molecular systems, from the simpler diatomics where Z_{eff} values are already found to be larger than the number of bound electrons [7], to the bigger polyatomic systems where Z_{eff} values up to five orders of magnitude larger than the total Z were observed [8,9]. Thus, it becomes very interesting, from a fundamental point of view as well as for the numerous applications of positron processes in molecular gases, to be able to provide some general explanation, at the nanoscopic level, for the findings on positron annihilation at room temperature. It is already clear that the uncorrelated dynamical picture implied by Eq. (1) is insufficient to explain the experimental observations, especially when the size of the molecules of the ambient gas increases [9]. An earlier phenomenological analysis of the data suggested an empirical linear scaling between the natural logarithm of Z_{eff} with the atomic ionization potentials minus the E_{ps} formation energy of 6.8 eV [10], hence conjecturing that a highly correlated electron-positron pair is created and moves in the field of the resulting molecular ions. Simple empirical relations between measured Z_{eff} values and molecular properties have been surmized and critically analyzed in recent work [9,10,11]. Additional studies [12] of polyatomics have put forward phenomenological modelings that consider two chief mechanisms.

(i) Direct annihilation of the incoming positron with one of the molecular electrons, a process dominant for atoms and small molecules and possibly related to the existence of low-lying, virtual states of a weakly bound positron to the molecular target.

(ii) Enhanced annihilation that occurs when the impinging positron undergoes resonant capture within one of the vibrationally excited, Feshbach-type resonances of the (target $+e^+$) complex that are formed during the scattering process. This latter mechanism was suggested to dominate for large molecules and for systems with high densities of vibrational states. On the whole, however, very little work has been done from first principles to obtain Z_{eff} values for large molecules and employing the full interaction and quantum dynamics of the positron-molecule scattering process. Some earlier calculations of ours have examined diatomic molecules [13] (and a linear molecule like CO_2 [7]) agreeing reasonably well with the existing experimental data but still finding discrepancies with some of them. Da Silva, Germane, and Lima [14] have also analyzed with an *ab initio* method the case of acetylene but found values that still disagree with the experi-

*FAX: +39-6-49913305.
Email address: FAGIANT@CASPUR.IT
†Present address: Physics Department, Bhairab Ganguly College, Calcutta, 700056, India.

ments. In other words, the theoretical and computational treatment of positron annihilation processes for large, nonlinear polyatomics gases has not been attempted as yet using nonparametric methods and therefore our knowledge of the most likely molecular mechanism is still not securely founded on a rigorous, and physically convincing explanation.

The aim of the present work is therefore that of providing an *ab initio*, parameter-free, model for the quantum treatment of positron annihilation in small polyatomic gases at room temperature, with the hope of obtaining some insight on the molecular properties that are likely to control the process and correlate best with either observed or computed Z_{eff} values. Whenever possible, we will also carry out a comparison with experiments and therefore try to assess the reliability of our method. As we shall see below, no unique answer on the most likely mechanism comes out of our analysis but the dominance of specific molecular properties will be fairly clearly established by our calculations and will support, for most of the molecules examined, the direct mechanism mentioned before.

In the following Sec. II we will outline our quantum-dynamical treatment while Sec. III reports the computed quantities and compares them, whenever possible, with experiments. Section IV finally summarizes our present conclusions.

II. THE QUANTUM DYNAMICS

A. The theoretical model

When discussing the quantum dynamics of positron collisions with molecular systems at energies below the threshold for P's formation one wishes to know the following aspects of the process: (i) the anisotropic charge distributions of the molecular targets and the corresponding static interactions of their electronuclear structures with the impinging positron; (ii) the short-range and medium-range description of the electron-positron dynamical correlation, and (iii) the long-range behavior of the target response to the e^+ perturbation, i.e., the polarization potential. For simplicity we shall assume that the nuclear motion is for the moment decoupled from the positron dynamics during the scattering process and we shall compute the scattering attributes of the process within the fixed-nuclei (FN) approximation. This simplification will, of course, prevent us from testing in this study the possible presence of nuclear-excited Feshbach resonances [12], an alternative that will be considering in our future work.

The above three points, however, have to be taken into account to carry out the quantum dynamics. As in our previous work on positron-molecule scattering [16,17], the actual evaluation of the static interaction, $V_{\text{st}}(\mathbf{r}_p)$, is done by expanding the self-consistent-field (SCF) wave function of each target molecule at its equilibrium geometry (see below for details) around the molecular center of mass (c.m.) using symmetry-adapted angular functions that transform with the relevant irreducible representation (IR) of the molecular point groups to which each molecule belongs. The details of the actual procedure will be given in the following section. Below the threshold of *Ps* formation, and above it for the elastic component of the total integral cross sections, one of the most serious questions concerns the clarification of the role played by long-range polarization forces and by short-range dynamical correlation effects. The final cross sections, in fact, turn out to be very sensitive to the detailed handling of both of the above contributions, especially at energies below *Ps* formation [17].

The direct approach to the inclusion of positron-electron correlation usually involves an extensive configuration-interaction expansion of the target electronic wave function over a set of excited electronic states and possibly a further improvement by adding Hylleraas-type functions that can describe the positron within the physical space of the target electronic charge distribution [18]. Such expansions, however, are markedly energy dependent and usually converge too slowly to be a useful tool for general implementation to complex molecular targets, where truncated expansions need to be very large before they get to be realistic in describing correlation effects [19]. As a consequence, we have developed over the years more tractable global models that do not depend on empirical parameters but can be easily implemented via a simplified, local representation of the positron correlation-polarization interactions, $V_{\text{pcp}}(\mathbf{r}_p)$ [20,21].

To begin with, one should note that the asymptotic form of the above interaction is independent of the sign of the impinging charged particle and, in its simpler spherical form, is given by the well-known second-order perturbation expansion formula (in atomic units)

$$V_{\text{pcp}}(\mathbf{r}_p)=\sum_{l=1}^{\infty} -\frac{\alpha_l}{2r_p^{2l+2}}, \tag{2}$$

where r_p represents now the scalar positron distance from the molecular c.m., and the α_1 are the multipolar static polarizabilities of the molecule, which depend obviously on the nuclear coordinates and on the electronic state of that target. In most cases only the lowest order is kept in the expansion given in Eq. (2) and therefore the target distortion is viewed as chiefly resulting from the induced dipole contribution with the molecular dipole polarizability as its coefficient [22]. In particular, we will be including only the spherical component of the above tensor quantity, i.e., the α_0 term. The drawback of the above expansion, however, is that it fails to correctly represent the true short-range behavior of the interaction and does not contain any effect from both static and dynamic correlation contributions. Therefore, a while ago, in order to correct for such failures, we proposed [15,16,20,21] to use a local density-functional approximation whereby the dynamical correlation that dominates the short-range behavior of the $V_{\text{pcp}}(\mathbf{r}_p)$ in closed-shell molecular targets can be treated using a density-functional theory (DFT) approach within the range of the target electronic density and can be further connected with the asymptotic dipolar form of Eq. (2) in the long-range region by ensuring the physically correct continuous behavior of the V_{pcp} potential over its whole range of action.

We therefore describe the full $V_{\text{pcp}}(\mathbf{r}_p)$ interaction as given by two distinct contributions that are connected at a

distance r_p^c generated by the continuity constraints and not, therefore, as a dispensable parameter. [21]

$$V_{\rm pcp}(\mathbf{r}_p)=\begin{cases} V_{\rm corr}^{\rm DFT}(\mathbf{r}_p), & r_p \leqslant r_p^c \\ V_{\rm pol}(\mathbf{r}_p), & r_p > r_p^c. \end{cases} \quad (3)$$

As discussed earlier [16], the short-range correlation contributions in Eq. (3) can be included either by considering the correlation effects on a homogeneous electron gas without reference to the positron projectile, as presented in Ref. [23], or by explicitly considering the positron as an impurity within a homogeneous electron gas [24]. We have derived both forms of $V_{\rm pcp}$ and discussed their merits for several molecular targets in our earlier work: only the latter model will be employed here. The form based on the density-functional theory for an isolated positron as an impurity of the electronic cloud will therefore provide here the chosen $V_{\rm corr}^{\rm DFT}(\mathbf{r}_p)$ interaction [25]. It was first derived following the density-functional expression of Boronski and Nieminen [24] and we have further modified its behavior beyond the matching region ($r_p > 4.0a_0$) to smoothly extend it, as $r_p \rightarrow \infty$, via Eq. (3).

The total interaction potential is then given as the sum of the static and correlation-polarization potentials, the latter being given by Eq. (3) while the former is calculated exactly from the target electronic density [16],

$$V_{\rm tot}(\mathbf{r}_p)=V_{\rm st}(\mathbf{r}_p)+V_{\rm pcp}(\mathbf{r}_p). \quad (4)$$

The corresponding close-coupling (CC) scattering equations, in the single-center-expansion (SCE) formulation, are therefore given by the following expression:

$$\left\{\frac{1}{2}\frac{d^2}{dr_p^2}-\frac{l(l+1)}{2r_p^2}+E_{\rm coll}\right\}u_{hl}^{p\mu}(r_p) = \sum_{h'l'} V_{hl,h'l'}^{p\mu}(r_p)u_{h'l'}^{p\mu}(r_p), \quad (5)$$

where $E_{\rm coll}$ is the collision energy and the positron-continuum radial functions $u_{h'l'}^{p\mu}(r_p)$ are the required unknown quantities originating from the symmetry-adapted SCF form of the wave function of the scattered particle:

$$F_{p\mu}(\mathbf{r}_p)=\sum_{hl} r_p^{-1}u_{hl}^{p\mu}(r_p)X_{hl}^{p\mu}(\hat{r}_p). \quad (6)$$

Here $p\mu$ labels the relevant IR, with p describing the IR of the scattered positron and μ being one of its component. The $X_{hl}^{p\mu}(\hat{r}_p)$ are the generalized harmonics. The index h further labels a specific angular basis function for each partial wave contribution l in the pth IR under consideration. The coupling matrix element on the right-hand side (rhs) of Eq. (5) is then given by

$$V_{hl,h'l'}^{p\mu}(r_p)=\langle X_{hl}^{p\mu}|V_{\rm tot}(\mathbf{r}_p)|X_{h'l'}^{p\mu}\rangle. \quad (7)$$

The details of the angular products have been described before [26] and will therefore not be repeated here. Suffice it to say that, when using the static+correlation+polarizatic (SCP) interaction within the SCE formulation and the CC dynamical formalism of Eq. (5) the corresponding coupled-differential equations (CDE) are solved to yield rotationally summed, integral elastic cross sections for each contributing IR. The total cross section is therefore simply given as

$$\sigma_{\rm tot}(E_{\rm coll})=\sum_{p,\mu}\sigma_{p,\mu}^{el}(E_{\rm coll}). \quad (8)$$

The individual K-matrix elements, for each $p\mu$, will then provide the total elastic (rotationally summed) cross sections that include all contributing IR at the considered collision energy.

One should mention at this point that the above treatment does not include any contribution from the Ps formation. Considering that the first ionization potentials are often around 10 eV and that the binding energy of Ps is 6.8 eV, then one sees that the threshold for Ps formation in many systems is really only of a few eV, in most cases well below 10 eV. Despite many experimental attempts, however, very few accurate measurements of absolute cross sections for this process have become available to date for molecular targets. The general findings from the more recent experiments are that *Ps* formation in molecular systems usually peaks around 27–30 eV while its percentage value just above threshold varies significantly with the type of molecule [27]. Hence, considering that the measured $Z_{\rm eff}$ refer to a very low range of collision energies, we qualitatively expect that this exclusion in our model should not be very significant.

In the following analysis we will see how realistically the present modeling of the interaction, and its use within the quantum formulation of the scattering, can obtain total elastic cross sections for a broad range of polyatomic molecules of medium size below the threshold of Ps formation, or right above it. The comparison with the existing experiments will, in fact, reveal that the present *ab initio* modeling of the elastic scattering is able to yield dynamical observables in fair accord with the measured data. This is not an idle point since the calculation of $Z_{\rm eff}$, which is one of the main objects of the present study, is closely related to the evaluation of the scattering K matrix, as we shall show below, and therefore to the cross sections given by Eq. (8). If one considers, in fact, one of the mechanisms put forward to explain the anomalous $Z_{\rm eff}$ values in polyatomic molecules, i.e., the direct binary collision mechanism [12] (one of the main objects of the present study) one sees that it is closely related to the evaluation of the K matrix. It is the scope of the present study just to see how well the description of annihilation within a FN treatment of molecular motion can perform *ab initio* $Z_{\rm eff}$ estimates for the broad range of medium-size molecules discussed below.

B. The $Z_{\rm eff}$ calculation

As mentioned in the Introduction, the $Z_{\rm eff}$ parameter is a measure, at a given relative energy or for a given temperature of the ambient gas, of the effective number of electrons that take part in the annihilation process when the molecular target interacts with an impinging positron. According to earlier models [5,6], when the relative energy increases and the

Born approximation is expected to hold, the positron wave function is approximated by a plane wave impinging on a single-particle, free-electron wave function at a time. Hence $Z_{\rm eff}$ tends to Z, the number of bound electrons which are all treated as ''free'' electrons [6]. The actual physical situation of the interacting electrons bound in a molecular environment is however different from this simple picture and therefore $Z_{\rm eff}$ should be more properly defined as

$$Z_{\rm eff}(k|\mathbf{R}) = \sum_{i=1}^{Z} \int d\mathbf{r}_1, \cdots d\mathbf{r}_Z \times \delta(\mathbf{r}_i - r_p) |\Psi_0(\mathbf{r}_1 \cdots \mathbf{r}_Z, \mathbf{r}_p|\mathbf{R})^2 d\mathbf{r}_p, \quad (9)$$

where the nuclear coordinate $\mathbf{R}$ is temporarily considered as a fixed parameter in the FN approach, $\mathbf{r}_i$ labels each electronic coordinate of the molecule and Z is the number of bound electrons in the target. Ψ_0 is the total wave function of the full system (Z electrons, M nuclei, one positron) which, at the simplest level of description, could be written as

$$\Psi_0(\mathbf{r}_1 \cdots \mathbf{r}_Z, \mathbf{r}_p|\mathbf{R}) = \chi_0(\mathbf{r}_1 \cdots \mathbf{r}_Z|\mathbf{R}) \varphi(\mathbf{r}_p|\mathbf{R}), \quad (10)$$

where we are considering for the moment only the normalized electronic ground state of the target molecule χ_0 and φ is the single-positron continuum function. One can further write

$$Z_{\rm eff}(k|\mathbf{R}) = \int d\mathbf{r}_p \rho(\mathbf{r}_p|\mathbf{R}) |\varphi(\mathbf{r}_p|\mathbf{R})|^2, \quad (11)$$

where

$$\rho(\mathbf{r}_p|\mathbf{R}) = Z \int |\chi_0(\mathbf{r}_1, \mathbf{r}_2 \cdots \mathbf{r}_Z|\mathbf{R}; \mathbf{r}_p)|^2 d\mathbf{r}_1, d\mathbf{r}_2 \cdots d\mathbf{r}_Z \quad (12)$$

is the target electron density evaluated at the same point in space where the positron is considered to be located $\mathbf{r}_p$ and provides the probability distribution for finding any of the electrons and the positron at the annihilation position. Here the target wave function is written down as a single-determinant (SD), expanded over the occupied one-particle molecular orbitals (MOs), and normalized so that $|\chi_0|^2$ integrated over all space is equal to unity.

It is important to remark at this point that the simplified expansion (10) merely indicates that, within the present treatment, the electronic target wave function does not undergo any excitation into different final electronic states after the positron leaves the system. In other words, it simply tells us that the annihilation process we are considering in our model will not cause permanent electronic excitations of the target after its occurrence. However, since this is too simple a physical picture, we have shifted into the computation of the continuum positron scattering states the effects of the target response to it, as discussed below.

The continuum function $\varphi(\mathbf{r}_p|\mathbf{R})$, which is part of it [see Eq. (10)], in fact, refers here to the scattered positron under the *full* action of the force field created by the molecular electrons and by their response to the impinging projectile as given in the preceding section. Hence, the scattering event is described by our model as realistically as possible and indeed includes the target distortion during the collision process to the extent that it is realistically provided by the $V_{\rm pcp}$ model potential discussed above Eq. (4). Furthermore, the multiple cusp features expected from the electron-positron correlated motion are here replaced by the DFT model suggested in [24], whereby the positron impurity is made to correlate with an homogeneous electron gas that has the density of our electronic target molecule.

Following the expansion (6), that FN form of the continuum positron can be used to describe a specific $|p\mu\rangle$ state of the scattered positron, the ensuing radial solution has therefore the following asymptotic form

$$u^{p\mu}_{hl,h'l'} \underset{r_p \to \infty}{\sim} A_{hl}\{\sin(kr_p - \tfrac{1}{2} l\pi)\delta_{hl,h'l'} + K_{hl,h'l'} \times \cos(kr_p - \tfrac{1}{2} l\pi)\}, \quad (13)$$

where the boundary conditions give us the A_{hl} normalization term [13].

A more general radial solution of the scattering problem is further given by

$$u_{h'l'}(r_p|\mathbf{R}) = \sum_{hl} a_{hl} u^{p\mu}_{h'l',hl}(r_p|\mathbf{R}), \quad (14)$$

since the coupled differential equations eventually yield a set of independent solutions labeled by $h'l'$. The coefficients a_{hl} are now chosen from the asymptotic form of the $\varphi(\mathbf{r}_p|\mathbf{R})$ of Eq. (11)

$$\varphi(\mathbf{r}_p|\mathbf{R})_{r_p \to \infty} e^{i\mathbf{k}\cdot\mathbf{r}_p} + f(\hat{\mathbf{k}}\cdot\hat{\mathbf{r}}_p)\frac{e^{i\mathbf{k}\cdot\mathbf{r}_p}}{r_p}. \quad (15)$$

The replacement of $\varphi(\mathbf{r}_p|\mathbf{R})$ into Eq. (10) via its asymptotic form of Eq. (15), and the further integration over $d\hat{\mathbf{k}}$ of the result, yields the following expression:

$$Z_{\rm eff}(k|\mathbf{R}) = \sum_{p\mu} Z^{p\mu}_{\rm eff}(k|\mathbf{R}), \quad (16)$$

where, for a target in its A_1 electronic state,

$$Z^{p\mu}_{\rm eff}(k|\mathbf{R}) = Z\frac{4\pi}{k^2} \sum_{\bar{h}''\bar{l}'',h''l''} \sum_{\bar{h}'\bar{l}',h'l'} \sum_{hl} (1+K^2)^{-1}_{\bar{h}''\bar{l}'',h''l''} g^{p\mu}_{hl} \times (h'l', \bar{h}'\bar{l}') s^{p\mu}_{hl}(h'l', h''l'', \bar{h}'\bar{l}', \bar{h}''\bar{l}'') \quad (17)$$

here K is the scattering K matrix of which the $h'l', h''l''$ element is indicated, the g's are the angular coefficients related to the potential terms of Eq. (7) (see Ref. [13]) and the s's are defined (always for the A_1 symmetry) as follows:

$$s^{p\mu}_{hl}(h'l', h''l''', \bar{h}'\bar{l}', \bar{h}''\bar{l}'') = \int_0^\infty b^{\Gamma}_{hl}(r_p|\mathbf{R}) u^{p\mu}_{h'l',h''l''}(r_p|\mathbf{R}) u^{p\mu}_{\bar{h}'\bar{l}',\bar{h}''\bar{l}''}(r_p|\mathbf{R}) dr_p \quad (18)$$

and the b's come from an additional multipolar expansion of the target electronic density of Eq. (12), taken to belong to the A_1 symmetry

$$\rho_{A_1}(\mathbf{r}_p|\mathbf{R}) = \sum_{hl} b_{hl}^{A_1}(r_p|\mathbf{R}) X_{hl}^{A_l}(\hat{\mathbf{r}}_p|\mathbf{R}). \tag{19}$$

Since the quantities that are experimentally measured usually come from averaging over the positron-velocity distribution v the final evaluation of $Z_{\text{eff}}(k)$ from Eq. (9) now needs to be further convoluted over a Boltzmann-type distribution function, $f(v|T)$ to obtain a temperature T dependence of the annihilation parameter

$$Z_{\text{eff}}(T|\mathbf{R}) = \int_0^\infty Z_{\text{eff}}(k|\mathbf{R}) f(v|T) dv, \tag{20}$$

from which one gets

$$Z_{\text{eff}}(T|\mathbf{R}) = \frac{4A^{3/2}}{\sqrt{\pi}} \int_0^\infty Z_{\text{eff}}(k|\mathbf{R}) k^2 \exp(-Ak^2) dk, \tag{21}$$

where, in atomic units:

$$A = \frac{1}{2k_B T}, \tag{22}$$

with k_B the Boltzmann constant.

Finally, since we have also seen that in the high energy limit the annihilation process should approach the Dirac estimate of the actual number of target electrons [6], we can further introduce an asymptotically normalized annihilation rate

$$Z_{\text{eff}}^N = \frac{Z_{\text{eff}}(T)}{Z}, \tag{23}$$

which allow us to quickly assess the departure of the molecular gas behavior to positron annihilation from its simpler asymptotic limit of the independent electron picture for its bound molecular electrons.

In the following analysis we shall try to see more in detail that: (i) the present modeling of the positron-molecule interaction appears to yield realistic estimates of the elastic integral cross sections for positron scattering from ambient molecular gases with polyatomic components at energy below the *Ps* formation threshold; (ii) the ensuing calculations for Z_{eff} values as a function of the ambient temperature reveal a fairly clear correlation with the molecular properties of the gases examined, although it is not entirely clear as yet which would be the chief nanoscopic cause of the large values; (iii) the use of the FN approximation, albeit simpler from the computational standpoint, decouples the positron dynamics from the molecular rovibrational states and therefore excludes for the moment the possibility of considering resonant-annihilation mechanisms [12]; and (iv) the study therefore focuses on the direct-annihilation mechanism and examines its validity for a broad range of small, nonlinear polyatomic gases.

III. COMPUTED AND MEASURED OBSERVABLES

As mentioned in the preceeding section, the present calculations have followed as much as possible a fully *ab initio* approach, in the sense that we have always solved the full-quantum-coupled equations for the dynamics, generating K-matrix elements to attain both the elastic cross sections for a variety of small polyatomic targets and to construct, via such elements, the annihilation process in the form of the dimensionless Z_{eff} parameter as a function of temperature. On the other hand, the collision dynamics was treated within the fixed-nuclei scheme and therefore no dynamical coupling with molecular rotovibrational degrees of freedom has been included. Furthermore, the positron-molecule interaction did not include the *Ps* formation channels and the e^+-e^- dynamical correlation was treated through a model, local interaction within a DFT scheme [13,20,21].

The dipole polarizabilities employed (as well as the molecular geometries) were always those known experimentally.

A. The computed cross sections

A first comparison could be obtained by computing the low-energy elastic cross sections and the corresponding Z_{eff} as a function of collision energy. We have therefore calculated both quantities using the same code and implementing the SCE of the bound and continuum particles (electrons and scattered positron, respectively) at the same level of numerical convergence. Thus, all the target wave functions were treated as near-Hartree-Fock SD's expanded over multicenter Gaussian orbitals (GTO's) at the molecular equilibrium geometries. The basis sets employed were those given by the GAUSSIAN 98 package [28]. The bound MO's were expanded up to $\lambda_{\max}$ values ranging from 10 to 50, ensuring convergence of the statistic potential terms within about 2–5%. Likewise, the potential multipoles were expanded up to twice the relevant $\lambda_{\max}$ value and the scattering wave function of the positron was expanded up to $\lambda_{\max}$ values that yielded K-matrix elements converged within 5%. All the details for the target properties and the scattering calculations are given in Table I.

The results shown in Fig. 1 report the computed cross sections of three molecular gases for which experimental total cross sections were also available: those for CH_4 from Ref. [29], those for NH_3 from Ref. [30], and those for H_2O are from [31]. The comparison between our computed (solid lines) and experimental data (filled in circles) clearly show that the calculations of the scattering observables yield values that are all reasonably close to the experimental data, with the exception of H_2O, where the calculations increase with decreasing collision energy much more rapidly than the experimental data. The role of permanent dipole moment of water, however, was not properly corrected in our body-fixed treatments, as is well known to be needed for polar targets [32]. This effect is particularly important at low collision energies and for systems with larger dipole moments, as is the case for water. On the other hand, the present treatment for nonpolar targets could be seen to be fairly realistic when compared with experiments. In Fig. 2, we show, in fact, the computed and measured elastic integral cross sections for

TABLE I. Some properties of the set of molecules examined in this work and details of the scattering calculations (all values in a.u.). [GTO, Gaussian orbital basis set. E_{SCF}, equilibrium energy from SCF calculations. SCE, λ_{max} of the MO's single-center expansions. MCOP, multipolar coefficients of the static potential ($2\lambda_{max}$). PPWE, λ_{max} for the positron partial wave expansions. μ, molecular permanent dipole moments (Debye).]

Molecule	GTO	E_{SCF}	SCE	MCOP	PPWE	μ
H_2O	cc-pVTZ	−76.061	12	24	12	1.8473
H_2S	D95**	−398.646	12	24	12	0.978
O_3	D95($3df,p$)	−224.329	36	72	12	0.534
SO_2	D95**	−547.203	36	72	12	1.633
NH_3	D95**	−56.209	42	84	12	1.47
PH_3	6-311^{++}G	−342.478	24	48	10	0.574
AsH_3	6-311^{++}G**	−2235.877	10	20	10	0.16
CH_4	D95	−40.185	12	24	12	
SiH_4	D95**	−291.230	20	40	20	
GeH_4	6-311G	−2077.607	20	40	20	
CF_4	D95*	−435.765	45	90	12	
SiF_4	D95*	−687.053	45	90	12	
CCl_4	D95*	−1875.720	45	90	12	
SF_6	6-311G($2d,2p$)	−994.220	42	84	12	

CF_4 (from Ref. [33]) and for SF_6 (from Ref. [34]). In both cases we see that the multielectron nature of the two target gases yield larger cross sections than in the case of CH_4, the effect being even more marked for SF_6 where our results suggest very large values, larger than those found for CF_4. Further tetrahedral target molecules are shown in Fig. 3, where we report the elastic cross sections for GeH_4, CCl_4, and SiF_4. The target with the largest number of electrons, CCl_4, shows indeed the largest elastic cross sections. The latter appear to be much larger than those shown by the SiF_4 molecule, a possible reason for which may be related to the more diffuse electronic density of the external chlorine atoms with respect to the more compact fluorine atoms. The distinct behavior of fluorinated compounds will be further discussed below when we shall analyze the values found for their Z_{eff} coefficients.

Further computed cross sections are shown in Fig. 4 for systems where, unfortunately, no experimental data could be found for comparison. The cross sections are now seen to be very large indeed for all the molecular targets reported on both panels. One further notices the enhancing effects produced by the permanent dipole moments: the SO_2 molecule yields the largest cross sections, while both PH_3 and AsH_3 (where only H atoms are located away from the expansion

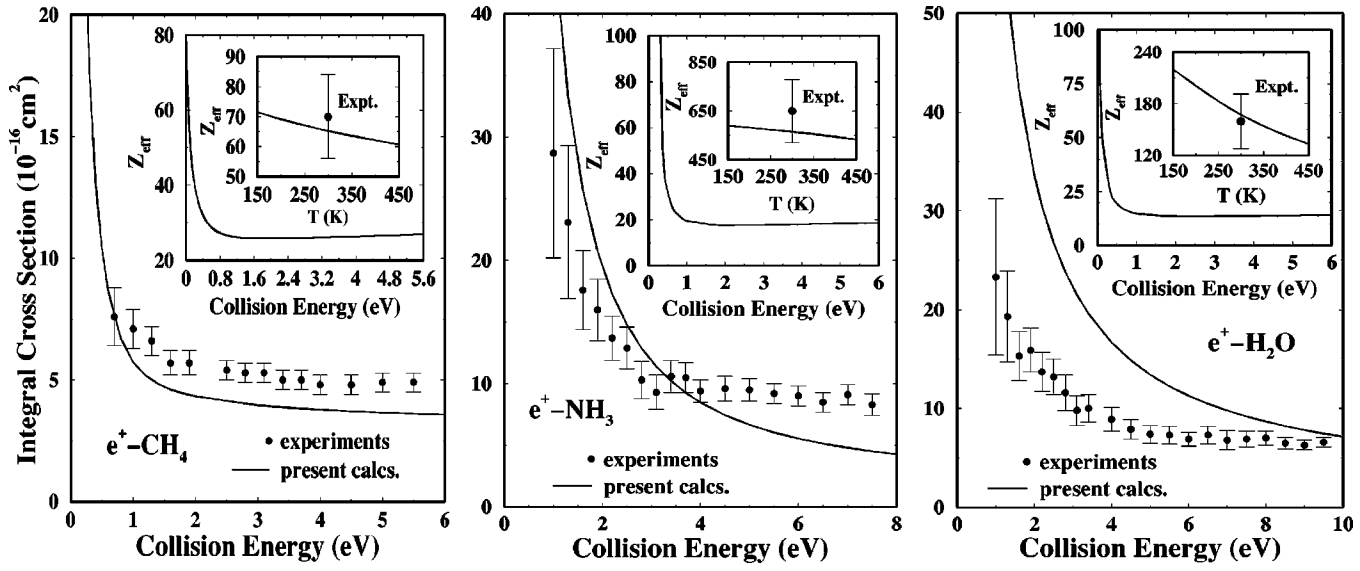

FIG. 1. Computed (elastic) and measured (total) cross sections for positron scattering from methane (left panel), from ammonia (middle panel), and from water (right panel). The experimental data are, from left to right: Refs. [29,30,31]. The inset shows the energy and temperature behavior of the annihilation rates, Z_{eff}. The experiments, from left to right, are from Refs. [2,8,9]. Their values have been multiplied by 0.5.

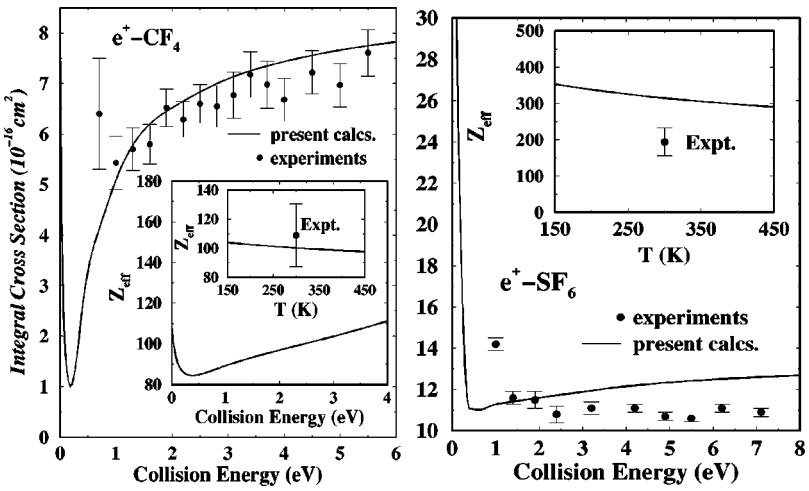

FIG. 2. Same quantities as in Fig. 1] but for carbon tetrafluoride (left panel) and for sulfur hexafluoride (right panel). The experimental total cross sections are from Refs. [33] and [34], while the experimental Z_{eff} values are from Refs. [2, 8,9. They have been mulitplied by 2.0.

centers) show smaller cross sections, as is also the case for the O_3 molecule that has a fairly small value (0.53 D) for its permanent dipole moment.

B. The computed annihilation parameters

The corresponding values of the annihilation parameters Z_{eff} are also shown for all the molecules reported in Figs. 1–4, where their temperature dependence is given and where, whenever possible, the existing experimental values are also shown for comparison. The actual numerical values at 300 K are reported in Table II for all the molecules examined in the present work.

The following comments could be made from a perusal of the results.

(i) The temperature dependence of all the computed Z_{eff} values shows a decrease as T increases.

(ii) From some molecular gases we also report the Z_{eff} dependence on collision energy. We see for all systems a dramatic drop of the values over the very-low range of energy ($\leqslant$1.0 eV). This effect suggests that the slower positron projectiles can more efficiently undergo multiple scattering within the spatial region of the target electron densities, thereby making the annihilation process more efficient, at least for the systems where it appears that the direct-annihilation mechanism discussed before [12] is the dominant one.

(iii) For all the molecular gases studied here the Z_{eff} are found to be larger than the corresponding total Z value of each individual molecule (see Table II). This result suggests, therefore, that the FN modeling, which we have used, and which implies the direct-annihilation mechanism to be the only possible one, indicates already an efficient annihilation behavior of the most of molecules examined, in agreement with the experiments.

(iv) The comparison with the available experiments is shown in Fig. 1 for H_2O, NH_3 and CH_4. The measured values have been halved in order to make them fit on the same scale of those computed. The experimental error bars are also reported [2,4,8,9]. It is interesting to note that the NH_3 molecule shows the largest measured Z_{eff} at 300 K and our calculations confirm this finding. Hence, in spite of the calculated values being smaller than those measured for all three molecules, we find that our model yields data that have the same order of magnitude of the experiments and give the same relative ordering along the series of molecules.

(v) We further see that the two fluorinated gases reported in Fig. 2 yield fairly small Z_{eff} values, only slightly larger than their corresponding total Z: the SiF_4 molecule of Fig. 3 shows a Z_{eff}/Z ratio of only 1.86. Such findings are in keeping with the experiments available for other fluorinated compounds [8,9]. We see, in fact, in Fig. 2 that the measured values for CF_4 and SF_6 need now to be multiplied by 2 or 3 in order to be on the same scale of the calculations. In other words, experiments tell of a marked quenching of the annihilation efficiency when the molecular target contains fluorine atoms [9,12]: our present calculations also follow the same behavior as we see from the data in Figs. 2 and 3.

(vi) The Z_{eff} calculations for the CCl_4 gas, on the other hand, indicate that our results are about nine times smaller than the experiments. This finding suggests that for the CCl_4

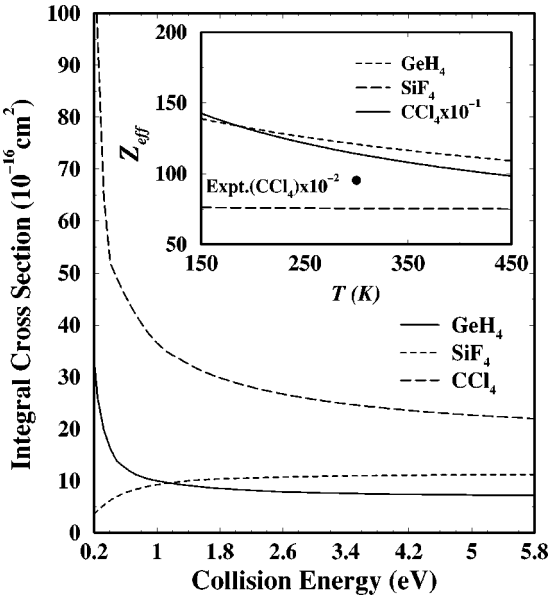

FIG. 3. Same as in Figs. 1 and 2 but for three different molecular gases: CCl_4 (solid lines), GeH_4 (short dashes), and SiF_4 (long dashes). The experimental value of Z_{eff} is from Ref. [9].

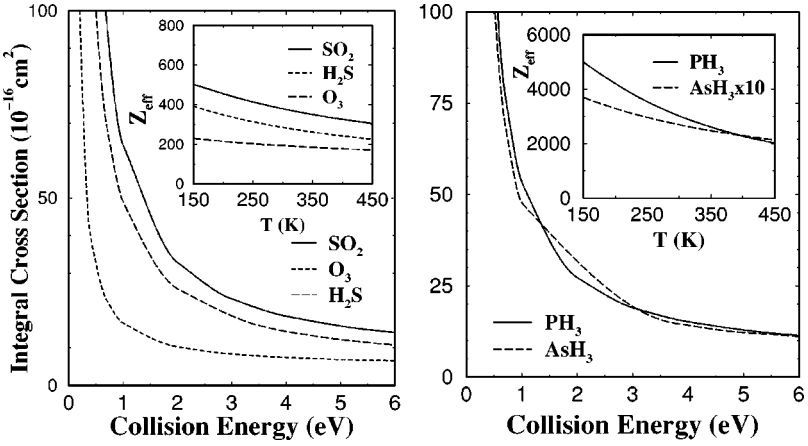

FIG. 4. Same as in Fig. 1 but for a different set of molecules. Only calculated results. Left panel: SO_2 (solid lines), O_3 (short dashes), H_2S (long dashes). Right panel: PH_3 (solid line) and AsH_3 (long dashes).

molecule, with the highest density of vibrational states per unit of energy, our model presumably describes incorrectly the mechanism for its annihilation rate when the FN approximation is employed. In other words, the marked enhancement of the Z_{eff} value of this gas suggests that the direct-annihilation mechanism should be replaced here by some other, more efficient, resonant-coupling dynamical mechanism that is not included within our modeling. Hence the marked underestimation of the experimental rates by our computation.

(vii) With the exception of the fluorinated molecules, the results for the multielectron gases shown in this work (see Table II) indicate nearly always enhancement of Z_{eff} with respect to their corresponding total Z values although the ratio ranges from about 167 for PH_3 to only 4 for GeH_4. In other words, all cases suggest that the efficiency of the direct mechanism can vary markedly with the microscopic structural properties of the relevant molecule in the gases. Below we therefore shall try to analyze in detail such correlation by trying to link the computed parameters to specific molecular features.

IV. CORRELATING Z_{eff} TO MOLECULAR PROPERTIES

As mentioned in previous sections, the molecules analyzed in the present work do not exhibit the orders-of-magnitude increase of Z_{eff} that have been experimentally detected in, say, the larger hydrocarbons [5,8,9]. Thus, the FN calculations suggest (with one exception) that the direct-annihilation mechanism is the most likely to act in the molecular gases that we have examined here. What we found in that analysis is also a marked dependence of the Z_{eff} values on the characteristics of the molecular gas, i.e., the variations of Z_{eff} along the series of molecules do not follow a simple pattern, although clearly showing to be very much molecule dependent.

In Fig. 5 we have collected the molecules that belong to the tetrahedral symmetry point group T_d and have shown in the four panels of the figure how the computed Z_{eff} values behave as a function of: (a) total Z, (b) the spherical dipole polarizabilities of the target α_0, (c) the energy threshold for *Ps* formation E_{PS}, and (d) the equilibrium distances R_{eq} between the central atom and the outer atoms in each molecule.

TABLE II. Computed and measured annihilation rates for the set of molecules examined in this work. See text for meaning of symbols. [$\delta Z_{\text{eff}}=(Z_{\text{eff}}^{\text{th}}-Z)/Z$ and $\Delta Z_{\text{eff}}=(Z_{\text{eff}}^{\text{exp}}-Z_{\text{eff}}^{\text{th}})/Z_{\text{eff}}^{\text{exp}}$. The percentage error for the quoted $Z_{\text{eff}}^{\text{exp}}$ values [8,9] is $\pm 20\%$.]

Mol	Z	$Z_{\text{eff}}^{\text{th}}$	$Z_{\text{eff}}^{\text{th}}/Z$	$Z_{\text{eff}}^{\text{expt}}/Z$	$Z_{\text{eff}}^{\text{exp}}\pm\Delta Z_{\text{eff}}^{\text{exp}}$	α_0 (a.u.)	E_{P_s} (eV)	R_{eq} (Å)	δZ_{eff}	ΔZ_{eff}
H_2O	10	167.22	16.72	31.9	319 ± 63.8	9.78	5.81	1.81	15.72	0.48
H_2S	18	285.17	15.84			25.51	3.65	1.42	14.84	
O_3	24	193.14	8.04			21.66	5.63	1.28	7.05	
SO_2	32	378.93	11.84			26.32	5.52	1.42	10.84	
NH_3	10	564.82	56.48	130	1300 ± 260	15.25	3.36	1.001	55.48	0.57
PH_3	18	3020.1	167.78			32.66	3.07	1.407	166.78	
AsH_3	36	269.66	7.49			25.95	3.78	1.497	6.49	
CH_4	10	64.7	6.47	14	140 ± 28	17.56	5.71	1.083	5.47	0.55
SiH_4	18	102.42	5.69			30.40	4.85	1.480	4.69	
GeH_4	36	120.78	3.35			34.40	4.53	1.530	2.35	
CF_4	42	98.5	2.34	1.29	54.4 ± 10.8	19.60	9.40	1.319	1.35	-0.81
SiF_4	50	75.41	1.51			19.40	8.90	1.560	0.87	
CCl_4	74	1140.6	15.41	128.78	9539 ± 1906	70.50	4.67	1.766	14.41	0.88
SF_6	70	319.93	4.49	1.38	97 ± 19	44.13	8.53	1.560	3.57	-2.29

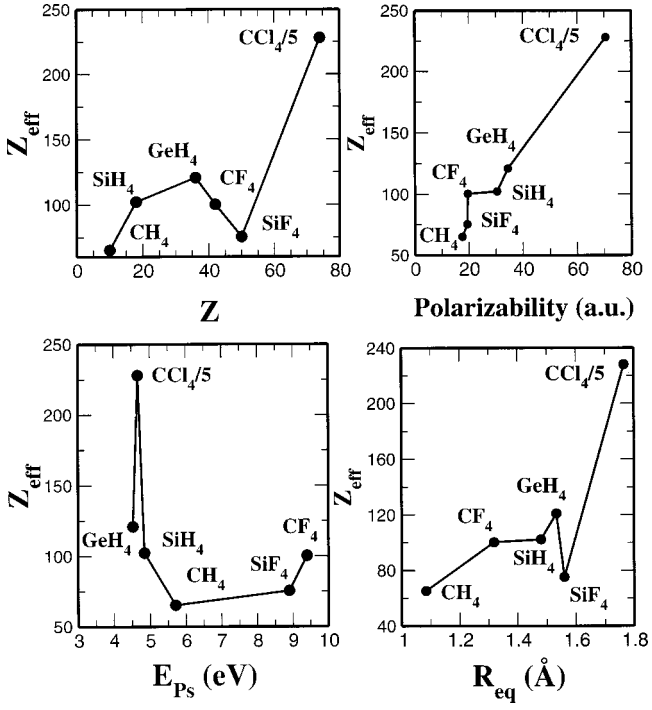

FIG. 5. Behavior of the computed Z_{eff} values in tetrahedral molecules as a function of different molecular properties. The data shown in each panels are correlated with the experimental values of each property.

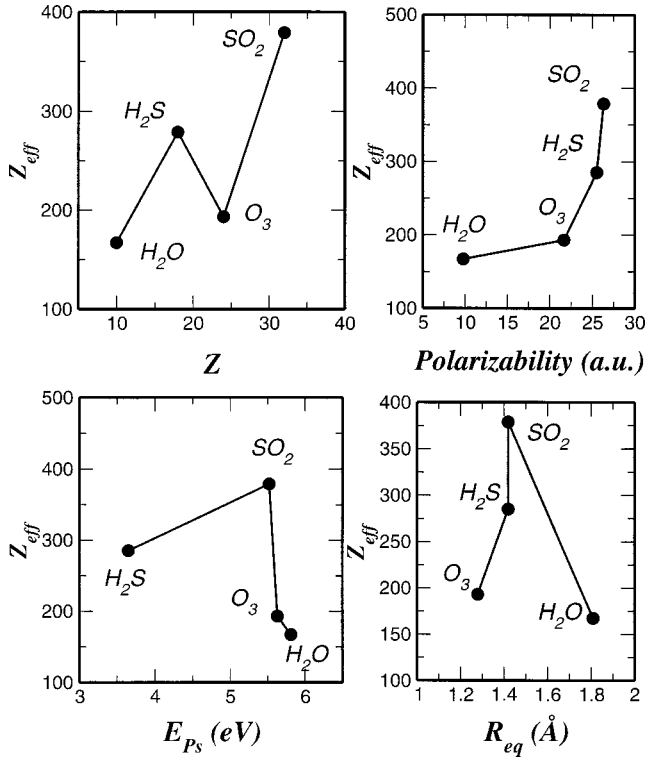

FIG. 6. Same correlation diagrams as in Fig. 5 but for molecules of C_{2v} symmetry.

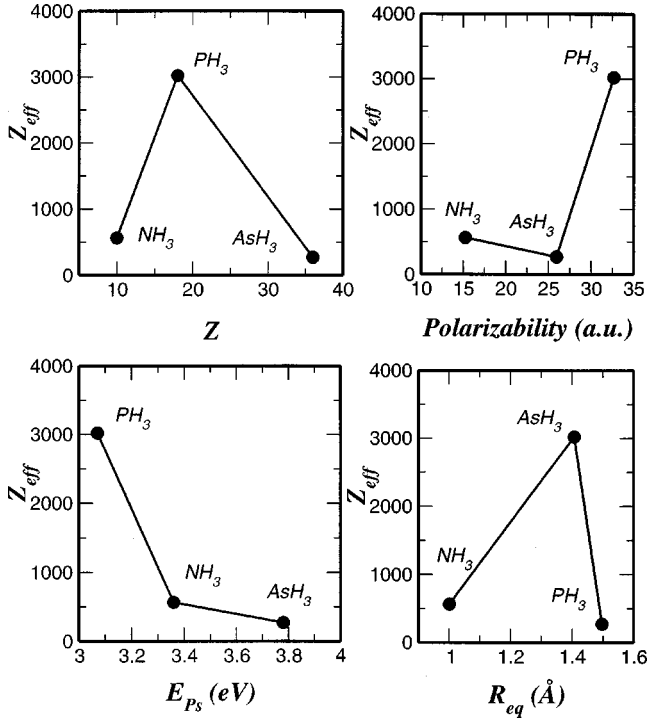

FIG. 7. Same correlation diagrams as in Fig. 5 but for molecules of C_{3v} symmetry.

The following findings are worth mentioning.

(1) All molecules appear to have annihilation parameters larger than their Z values. They also show the lowest Z_{eff}/Z ratios for the fluorinated gases and the largest ratio for the CCl_4 molecule (upper left panel).

(2) Both the polarizability values and the size of the R_{eq}'s (directly related to the electronic density spatial extension) clearly indicate CCl_4 the candidate gas for the largest annihilation parameter values, as indeed found experimentally [4,9].

(3) The Ps energy thresholds suggest that the fluorinated compounds should have the least efficient annihilation kinetics, as found by the measurements, while the behavior of the CCl_4 target gas indicates that its kinetics is probably controlled by a different molecular mechanism from the one we have employed in this study.

That the molecular symmetries could be a possible correlation parameter is also shown by the results presented in Figs. 6 and 7, where we have gathered the same Z_{eff} dependence seen in Fig. 5 but this time for the polar targets of C_{2v} symmetry (Fig. 6) and of C_{3v} symmetry (Fig. 7).

We see there that the less symmetrical situations indeed blur the overall picture and make it more difficult to identify simple patterns. For instance, the Z_{eff}/Z ratios become, broadly speaking, larger than those for the T_d molecules: a factor of about 2 for the C_{2v} set and of about one order of magnitude for the C_{3v} group, with the exception of the AsH_3 case.

One further gathers from the last two figures that the dipole polarizability plays an important role and clearly correlates, as in the T_d group, with the computed Z_{eff}. The role of energy thresholds and of molecular electron density ''vol-

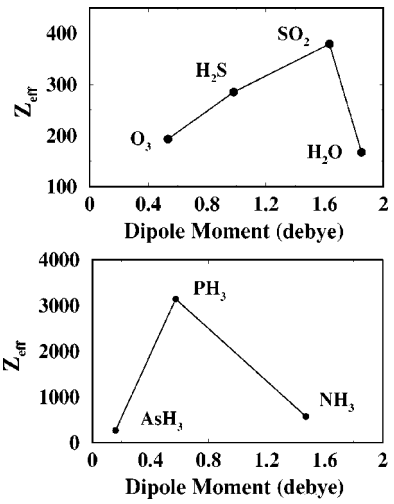

FIG. 8. Correlation between computed annihilation rates (at 300 K) and molecular dipole moments. Top panel: C_{2v} molecules. Lower panel: C_{3v} molecules.

umes'' is, however, not as clear as before.

Since the C_{2v} and C_{3v} symmetries refer to polar gases, it is of some use to try to correlate the computed annihilation efficiency with their permanent dipole moments, as shown in Fig. 8. Both panels indicate only a qualitative correlation between Z_{eff} and μ but not any straightforward increase of annihilation rates as the molecular dipole increases. As a matter of fact, the experimental Z_{eff} for ammonia turns out to be about four times that of water, while the magnitudes of their permanent dipole moments are very similar (see Tables I and II).

A further attempt at correlating the computed parameters with some molecular property common to all the molecular symmetries we have studied here is given in Fig. 9, where the compounds examined are grouped by symmetry to show the dependence of their Z_{eff} values on their corresponding spherical dipole polarizabilities. The correlation is now much

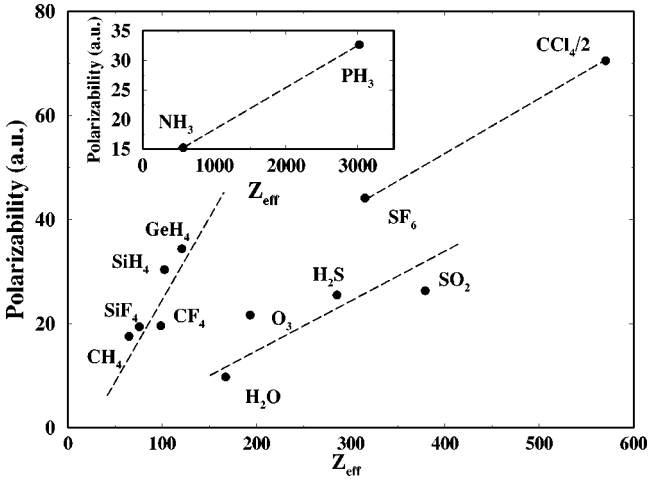

FIG. 9. Correlation diagram between computed Z_{eff} values (at 300 K) and experimental molecular dipole polarizabilities (spherical terms). The molecules are grouped together by their point-group symmetries, as shown in previous figures.

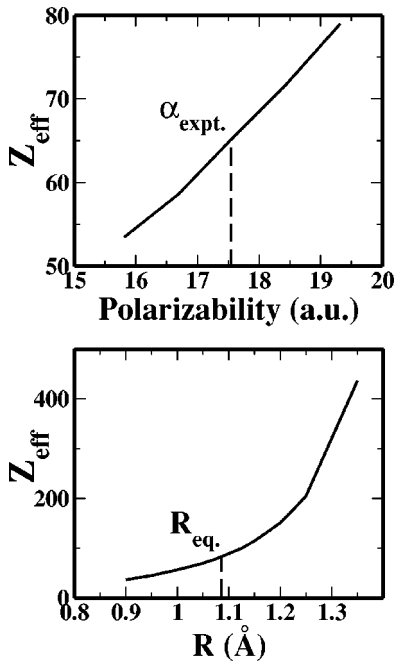

FIG. 10. Computed Z_{eff} dependence on two molecular properties for the case of the CH_4 molecular gas. Upper panel: changes of annihilation rates as a function of the dipole polarizability values. Lower panel: changes of the computed Z_{eff} as a function of the $R_{C\text{-}H}$ distances in the tetrahedral structure.

clearer and we see that, within each group of molecule, the largest Z_{eff} values go with the target that has the largest dipole polarizability. It is interesting to also note that the CCl_4 molecule shows one of the largest values for both quantities but still a marked discrepancy with experiments (see Fig. 3). Thus, its large α_0 value at equilibrium geometry could also point at possible large effects coming from low-energy vibrational couplings dynamics, as we shall briefly discuss below.

A possible alternative mechanism suggested to occur for the cases where Z_{eff} reaches much larger values than those discussed here is that of its enhancement through vibrationally excited core resonances induced by some more efficient positron trapping [9,12].

A simple numerical model for the above effect is reported in Fig. 10, where we show in the upper panel the changes of Z_{eff} at room temperature, for the methane molecule, when its dipole polarizability is arbitrarily varied from its experimental value, also marked in the figure. One sees there that contained variations of α_0 (by about 20%) can cause Z_{eff} variations of the same order of magnitude, i.e., not particularly dramatic. On the other hand, the lower panel in the same figure shows that, when the molecular ''size'' is varied by changing the $R_{C\text{-}H}$ distance (with its experimental value also marked in the figure) of about the same amount, the corresponding Z_{eff} calculated at the different T_d geometries (only the breathing mode was considered, for simplicity) varies by nearly one order of magnitude. This startling result indicates that, at least for nonlinear polyatom gases, the inclusion of nuclear motion effects could drastically modify the Z_{eff} values and could help to explain the different behavior of the CCl_4 gas. With the same token, and considering the fair ac-

cord with experiments afforded by the FN calculations for methane (see Fig. 1), we can also suggest that resonance effects play a minor role in this case and that the direct mechanism is likely to be the dominant one for this gas and for nearly all the molecules examined here.

V. CONCLUSIONS AND OUTLOOK

In the present work we have analyzed, using quantum dynamics with parameter-free interaction potentials, the low-energy elastic scattering of positrons from polyatomic gases and their corresponding annihilation rates at room temperature. The set of molecules examined involves only nonlinear polyatomics of small and medium size, from 10-electron species (e.g., H_2O,CH_4,NH_3, etc.) up to carbon tetrachloride and sulfur hexafluoride.

The aim of this work was to test the validity of a quantum treatment in which the internal degrees of freedom associated with the nuclei (e.g., rotations and vibrations) and the permanent excitation of electronic states are essentially excluded from the dynamics. Furthermore, the correlation contributions from electron-positron interactions were included via a global DFT formulation at the local-density approximation level [24], a procedure already found by us to be qualitatively acceptable for calculating other scattering observables [35].

The evaluation of the elastic cross sections, in comparison with the available experiments, suggests that the present procedure is able to provide a fairly realistic representation of the scattering K-matrix elements, a key factor for the evaluation of the Z_{eff} rates in the molecular gases.

On the strength of this general agreement with available experiments, the ensuing evaluation of the annihilation rates allowed us to reach the following, albeit preliminary, conclusions.

(i) The calculated rates, in the cases where comparison with experiment was possible, turned out to be in qualitative agreement with existing data, with the exception of the CCl_4 gas.

(ii) The absence of including closed, Feschbach-type, vibrational channels in the scattering equations suggests that for most of the above gases the annihilation occurs via a direct process essentially driven by the targets' linear response to the perturbing projectile via its dipole polarizability.

(iii) The reduced rates for fluorinated compounds, a feature found both by experiments and by our calculations, is explained qualitatively by the greater electronegativity of the F atom that therefore reduces in size the electronic density and increases the electron localization near such nuclei. As a consequence of it, positron-annihilation samples a reduced spatial region with non-negligible electron population.

(iv) The strong enhancement of the Z_{eff} values for the CCl_4 gas in comparison with the experiments suggests that, at least for this system, the FN dynamics does not realistically describe the dynamical positron coupling with the molecular nuclei during the annihilation process. Hence, the present calculations indirectly suggest for this system an annihilation mechanism that might involve nuclear-excited close-channel resonances [12]. This conjecture is also suggested by the computed effect of nuclear geometry changes on enhancing Z_{eff} values, as seen from the test calculations on methane reported in Fig. 10.

On the whole, therefore, the still preliminary results from this study underline the crucial importance of including detailed analysis of the molecular properties when setting up a theoretical modeling for positron-annihilation rates in polyatomic gases. One should also note that a great deal of work still needs to be done on the full *ab initio* treatment of dynamical correlation effects for positron scattering and on the important issue of the binding properties of these molecular gases with low-energy positrons. Neither of the above features has been included here, where our aim has been to achieve a more heuristic description of the forces at play in order to provide, to our knowledge for the first time, a non-empirical account of the dynamics relevant to positron-annihilation processes in polyatomic molecules. The information gathered from the present findings is hopefully going to be important for guiding further developments in *ab initio* treatment of positron dynamics in polyatomic gases.

ACKNOWLEDGMENTS

The financial support of the Italian National Research Council (CNR), of the Ministry for University and Research (MURST), and of the Max-Planck Research Society is gratefully acknowledged. We are also grateful to Dr. Tamio Nishimura for a careful reading of the manuscript and for his several suggestions on the discussion of the present results.

[1] E.g., see *Annihilation* in *Gases and Galaxies*, edited by R. J. Drachman, NASA Conf. Publ. No. 3058 (NASA, Washington, DC, 1990).

[2] K. Iwata, R. G. Greaves, and C. M. Surko, Phys. Rev. A **55**, 3586 (1997).

[3] P. Van Reeth, J. W. Humbertson, K. Iwata, R. G. Greaves, and C. M. Surko, J. Phys. B **39**, L465 (1996).

[4] S. J. Gilbert, R. G. Greaves, and C. M. Surko, Phys. Rev. Lett. **82**, 5032 (1999).

[5] E.g., see J. W. Humbertson and J. B. G. Wallace, J. Phys. B **5**, 1138 (1972).

[6] P. A. M. Dirac, Proc. R. Soc. London, Ser. A **117**, 610 (1928); **118**, 351 (1928).

[7] F. A. Gianturco and T. Mukherjee, Europhys. Lett. **48**, 519 (1999).

[8] J. D. Mc Nutt and S. C. Sharma, J. Chem. Phys. **62**, 1777 (1975); D. A. L. Paul, Phys. Rev. Lett. **11**, 493 (1963).

[9] K. Iwata, R. G. Greaves, T. T. J. Murphy, M. D. Tinkle, and M. C. Surko, Phys. Rev. A **51**, 473 (1995); K. Iwata, G. F. Gribakin, R. G. Greaves, C. Kutz, and C. M. Surko, *ibid.* **61**,

022719 (2000).
[10] T. J. Murphy and C. M. Surko, Phys. Rev. Lett. **67**, 2954 (1991).
[11] T. Laricchia and C. Wilkin, Phys. Rev. Lett. **79**, 2241 (1997); J. Mitroy and G. G. Ryzhikin, *ibid.* **83**, 3570 (1999).
[12] G. F. Gribakin, Phys. Rev. A **61**, 022720 (2000).
[13] F. A. Gianturco and T. Mukherjee, Nucl. Instrum. Methods Phys. Res. B **171**, 17 (2000).
[14] E. P. Da Silva, J. S. E. Germane, and M. A. P. Lima, Phys. Rev. Lett. **77**, 1028 (1996).
[15] F. A. Gianturco and D. De Fazio, Phys. Rev. A **550**, 4819 (1994).
[16] F. A. Gianturco, A. Jain, and J. A. Rodriguez-Ruiz, Phys. Rev. A **47**, 1075 (1993).
[17] E.g., see T. L. Gibson, J. Phys. B **23**, 767 (1990).
[18] E. A. G. Armour, Phys. Rep. **169**, 1 (1988).
[19] R. N. Hewitt, C. J. Noble, and B. H. Brandsden, J. Phys. B **25**, 557 (1992).
[20] F. A. Gianturco and J. A. Rodriguez-Ruiz, Phys. Rev. A **47**, 1075 (1993).
[21] F. A. Gianturco, J. A. Rodriguez-Ruiz, and N. Sanna, Phys. Rev. A **52**, 1257 (1995).
[22] E.g., see M. A. Morrison, Adv. At. Mol. Phys. **24**, 51 (1988).
[23] F. A. Gianturco and R. Melissa, Europhys. Lett. **33**, 661 (1996).
[24] E. Boronski and R. M. Nieminen, Phys. Rev. B **34**, 3820 (1986).
[25] A. Jain, Phys. Rev. A **41**, 2437 (1990).
[26] F. A. Gianturco and A. Jain, Phys. Rep. **143**, 347 (1986).
[27] E.g., see D. Fromme, G. Kruse, W. Raith, and G. Sinapius, Phys. Rev. Lett. **57**, 3031 (1986).
[28] GAUSSIAN98, M. J. Frish, A. Frish, and J. B. Foresman (Gaussian Inc.).
[29] O. Sueoka and S. Mori, J. Phys. Soc. Jpn. **53**, 2491 (1984).
[30] O. Sueoka, S. Mori, and Y. Katayama, J. Phys. B **20**, 3237 (1987).
[31] O. Sueoka, S. Mori, and Y. Katayama, J. Phys. B **19**, L373 (1986).
[32] E.g., see F. A. Gianturco and P. Paioletti, in *Novel Aspects of Electron-Molecule Scattering*, edited by K. H. Becker (World Scientific, Singapore, 1998), p. 256.
[33] O. Sueoka, S. Mori, and A. Hamada, J. Phys. B **27**, 1453 (1994).
[34] M. S. Dababneh, Y.-F. Hsieh, W. E. Kauppila, C. K. Kwan, S. J. Smith, T. S. Stein, and M. N. Uddin, Phys. Rev. A **38**, 1207 (1988); O. Sueoka, H. Takaki, and A. Hamada, At. Collision Res. Jpn. **23**, 6 (1997).
[35] R. Curik, N. Sanna, and F. A. Gianturco, J. Phys. B **33**, 615 (1999).